

# Luminescence and Energy Transfer of Eu- and Mn-Coactivated $\text{CaAl}_2\text{Si}_2\text{O}_8$ as a Potential Phosphor for White-Light UVLED

Woan-Jen Yang,<sup>†</sup> Liyang Luo,<sup>‡</sup> Teng-Ming Chen,<sup>\*,†</sup> and Niann-Shia Wang<sup>‡</sup>

Phosphors Research Laboratory, and Institute of Molecular Science, Department of Applied Chemistry,  
National Chiao Tung University, Hsinchu 30050, Taiwan

Received March 24, 2005. Revised Manuscript Received May 16, 2005

A series of  $\text{Eu}^{2+}$ - and  $\text{Mn}^{2+}$ -coactivated  $\text{CaAl}_2\text{Si}_2\text{O}_8$  phosphors have been synthesized at 1400 °C under a reduced atmosphere and their luminescence properties have been investigated as a function of activator and coactivator concentrations. We have discovered that energy transfers from  $\text{Eu}^{2+}$  to  $\text{Mn}^{2+}$  by directly observing significant overlap of the excitation spectrum of  $\text{Mn}^{2+}$  and the emission spectrum of  $\text{Eu}^{2+}$  as well as the systematic relative decline and growth of emission bands of  $\text{Eu}^{2+}$  and  $\text{Mn}^{2+}$ , respectively. The critical distance and average separation of  $\text{Eu}^{2+}$  and  $\text{Mn}^{2+}$  have also been calculated. By utilizing the principle of energy transfer, we have also demonstrated that with appropriate tuning of activator content  $\text{CaAl}_2\text{Si}_2\text{O}_8:\text{Eu}^{2+},\text{Mn}^{2+}$  phosphors exhibit great potential to act as a phosphor for white-light ultraviolet light-emitting diodes (UVLEDs).

## 1. Introduction

It has been well-known that  $\text{Eu}^{2+}$  may act as an efficient sensitizer that transfers energy to  $\text{Mn}^{2+}$  in several host lattices.<sup>1,2</sup> For instance, Caldino et al. described the  $\text{Eu}^{2+} \rightarrow \text{Mn}^{2+}$  energy transfer process in  $\text{CaCl}_2:\text{Eu}^{2+},\text{Mn}^{2+}$  single crystals under photoexcitation. The authors suggested that the  $\text{Eu}^{2+}$  to  $\text{Mn}^{2+}$  energy transfer process observed in  $\text{CaCl}_2:\text{Eu},\text{Mn}$  can be rationalized by the formation of small complexes of  $\text{Eu}-\text{Mn}$  in the lattice.<sup>1</sup> Similar energy transfer was also observed by Barry in the  $\text{BaMg}_2\text{Si}_2\text{O}_7:\text{Eu}^{2+},\text{Mn}^{2+}$  phosphor.<sup>3</sup> Recently, Yao et al. reported the luminescence and decay behaviors of  $\text{BaMg}_2\text{Si}_2\text{O}_7:\text{Eu}^{2+},\text{Mn}^{2+}$  as a function of dopant concentrations and confirmed the presence of  $\text{Eu}^{2+} \rightarrow \text{Mn}^{2+}$  energy transfer.<sup>4</sup>

Rubio et al.<sup>5</sup> proposed an ionic radius criterion to predict pairing between two impurity dopant ions in alkali halide host matrices, which may provide a reasonable basis for selecting appropriate impurity dopant ions for developing efficient phosphor materials. Furthermore, the  $\text{Eu}^{2+} \rightarrow \text{Mn}^{2+}$  energy transfer mechanism in  $\text{KBr}:\text{Eu}^{2+},\text{Mn}^{2+}$  phosphor was described by Mendez et al.<sup>6</sup> who proposed the possible formation of small  $\text{Eu}^{2+}-\text{Mn}^{2+}$  clusters in the KBr lattice. Mendez et al. also indicated that the  $\text{Eu}^{2+} \rightarrow \text{Mn}^{2+}$  energy transfer can be explained by assuming that a dipole–

quadrupole or exchange (superexchange) interaction mechanism is active in the  $\text{Eu}^{2+}-\text{Mn}^{2+}$  cluster formation.<sup>6</sup>

Very recently, Kim et al. reported that  $\text{Ba}_3\text{MgSi}_2\text{O}_8:\text{Eu},\text{Mn}$  can be used as a phosphor for fabrication of a warm white-light emitting diode.<sup>7</sup> They concluded that with optimal excitation wavelength at 375 nm  $\text{Ba}_3\text{MgSi}_2\text{O}_8:\text{Eu},\text{Mn}$  was observed to show three emission bands centered at 442 nm (from  $\text{Eu}^{2+}$  and with decay time of 0.32  $\mu\text{sec}$ ), 505 nm (from  $\text{Eu}^{2+}$  and with decay time of 0.64  $\mu\text{sec}$ ), and 620 nm (from  $\text{Mn}^{2+}$  and with a decay time of 750  $\mu\text{sec}$ ),<sup>7</sup> respectively.

Despite the above-mentioned research on the luminescent properties and energy transfer of Eu and Mn-codoped materials, to the best of our knowledge, there have been no investigations regarding the luminescence in  $\text{CaAl}_2\text{Si}_2\text{O}_8:\text{Eu},\text{Mn}$  published, nor is the energy transfer between  $\text{Eu}^{2+}$  and  $\text{Mn}^{2+}$  in the host of  $\text{CaAl}_2\text{Si}_2\text{O}_8$  reported in the literature. Anorthite ( $\text{CaAl}_2\text{Si}_2\text{O}_8$ ) was reported to be crystallized in a triclinic crystal system with space group  $\bar{1}$  under ambient pressure by Angel in 1988.<sup>8</sup> In the crystal lattice, there are six crystallographically independent cation sites, namely, four  $\text{Ca}^{2+}$  sites, one  $\text{Al}^{3+}$  site, and one  $\text{Si}^{4+}$  site. One type of  $\text{Ca}^{2+}$  ion occupies an octahedral site with six oxygen atoms and the average  $\text{Ca}-\text{O}$  bond distance is 2.485 Å. Other  $\text{Ca}^{2+}$  ions occupy three kinds of polyhedral sites with seven coordinated oxygen atoms and their average bond distances are 2.508, 2.531, and 2.562 Å, respectively. Al and Si atoms both occupy tetrahedral sites with four coordinated oxygen atoms, and the average bond distances for  $\text{Al}-\text{O}$  and  $\text{Si}-\text{O}$  are 1.735 and 1.611 Å, respectively.<sup>8</sup>

Motivated by the above investigations and the attempt to develop phosphors excitable by ultraviolet radiation for the applications of white-light LED, we have investigated the

\* Corresponding author. E-mail: tmchen@mail.nctu.edu.tw. Tel: 886+35731695. Fax: 886+ 35723764.

<sup>†</sup> Phosphors Research Laboratory.

<sup>‡</sup> Institute of Molecular Science.

(1) Caldino, U. G.; Munoz, A. F.; Rubio, J. O. *J. Phys.: Condens. Matter* **1990**, *2*, 6071.

(2) Caldino, U. G.; Munoz, A. F.; Rubio, J. O. *J. Phys.: Condens. Matter* **1993**, *5*, 2195.

(3) Barry, T. L. *J. Electrochem. Soc.* **1970**, *117*, 381.

(4) Yao, G. Q.; Lin, J. H.; Zhang, L.; Lu, G. X.; Gong, M. L.; Su, M. Z. *J. Mater. Chem.* **1998**, *8*, 585.

(5) Rubio, J. O.; Murrieta, S. H.; Powell, R. C.; Sibley, W. A. *Phys. Rev. B* **1985**, *31*, 59.

(6) Mendez, A.; Ramos, F.; Rıceros, H.; Camarillo, E.; Caldino U. G. *J. Mater. Sci. Lett.* **1999**, *18*, 399.

(7) Kim, J. S.; Jeon, P. E.; Choi, J. C.; Park, H. L.; Mho, S. I.; Kim, G. *C. Appl. Phys. Lett.* **2004**, *84*, 2931.

(8) Angel, R. J. *Am. Mineral.* **1988**, *73*, 1114.

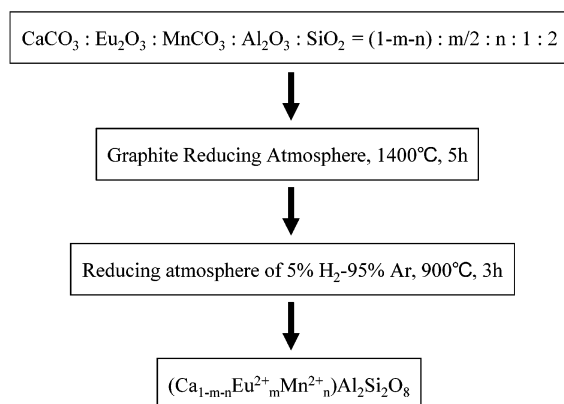


**Figure 1.** Flowchart diagram for the synthesis of  $\text{CaAl}_2\text{Si}_2\text{O}_8\text{:Eu,Mn}$  phosphors.

luminescence, energy transfer, and color chromaticity properties of  $\text{CaAl}_2\text{Si}_2\text{O}_8\text{:Eu,Mn}$  phosphor in the present work. We have also calculated the average separation between  $\text{Eu}^{2+}$  and  $\text{Mn}^{2+}$  ions ( $R_{\text{Eu-Mn}}$ ) in the host lattice as well as the critical distance ( $R_c$ ) between  $\text{Eu}^{2+}$  and  $\text{Mn}^{2+}$  ions for the occurrence of energy transfer based on the model proposed by Blasse.<sup>9</sup> Our investigation has demonstrated that  $\text{CaAl}_2\text{Si}_2\text{O}_8\text{:Eu,Mn}$  can emit white-light under ultraviolet excitation by systematically tuning the relative doping content of  $\text{Eu}^{2+}$  relative to that of  $\text{Mn}^{2+}$ .

## 2. Experimental Section

**2.1 Materials and Synthesis.** A series of polycrystalline  $(\text{Ca}_{1-m-n}\text{Eu}_m\text{Mn}_n)\text{Al}_2\text{Si}_2\text{O}_8$  (abbreviated as  $\text{CaAl}_2\text{Si}_2\text{O}_8\text{:Eu,Mn}$ ) samples investigated in this work were prepared by solid-state reactions and the synthetic procedure is summarized in Figure 1. Briefly, the constituent oxides or carbonates  $\text{CaCO}_3$  (99.99%),  $\text{Eu}_2\text{O}_3$  (99.99%),  $\text{MnCO}_3$  (99.99%),  $\text{Al}_2\text{O}_3$  (99.99%), and  $\text{SiO}_2$  (99.99%) (all from Aldrich Chemicals, Milwaukee, WI) were intimately mixed in the requisite proportions. The mixtures were first calcined and then sintered at 1400 °C for 5 h to avoid the inclusion of carbonate impurities. The obtained product was then reduced at 900 °C for 3 h under 5:95  $\text{H}_2/\text{Ar}$  atmosphere. The  $\text{Y}_3\text{Al}_5\text{O}_{12}\text{:Ce}$  (Catalog NP-204) sample used as a blue-LED convertible phosphor to generate white light in the Commission International de l'Eclairage (CIE) chromaticity investigations was obtained from Nichia Corporation, Japan.

**2.2 Characterizations.** The phase purity of the as-prepared phosphor samples was checked by powder X-ray diffraction (XRD) analysis with a Bruker AXS D8 advanced automatic diffractometer with  $\text{Cu K}\alpha$  radiation operating at 40 kV and 20 mA. The XRD profiles were collected in the range of  $10^\circ < 2\theta < 80^\circ$ . The measurements of photoluminescence (PL) and photoluminescence excitation (PLE) spectra were performed by using a Spex Fluorolog-3 spectrofluorometer (Instruments S.A., NJ) equipped with a 450-W Xe light source and double excitation monochromators. The powder samples were compacted and excited under  $45^\circ$  incidence and emitted fluorescence was detected by a Hamamatsu Photonics R928 type photomultiplier perpendicular to the excitation beam. The spectral response of the measurement

system is calibrated automatically on start up. To eliminate the second-order emission of the source radiation, a cutoff filter was used in the measurements.

The emission lifetime was measured by using a third harmonic (355 nm, pulse width  $\sim 10$  ns) of Nd:YAG laser (Continuum NY60). The emission signal passing through a monochromator (ARC spectraPro 300i) was detected by a photomultiplier tube (Hamamatsu 1P28) and was averaged by a digital oscilloscope (LeCroy LT372).

The reflectance spectra of the samples were measured with a Hitachi 3010 double-beam UV-vis spectrometer (Hitachi Co., Tokyo, Japan) equipped with a  $\phi 60$ -mm integrating sphere whose inner face was coated with  $\text{BaSO}_4$  or Spectralon and  $\alpha\text{-Al}_2\text{O}_3$  was used as a standard in the measurements. The Commission International de l'Eclairage (CIE) chromaticity coordinates for all samples were determined by a Laiko DT-100 color analyzer equipped with a CCD detector (Laiko Co., Tokyo, Japan).

## 3. Results and Discussion

Polycrystalline  $\text{CaAl}_2\text{Si}_2\text{O}_8\text{:Eu,Mn}$  phosphor samples used in this work have been synthesized at 1400 °C and then annealed under a reduced atmosphere of 5:95  $\text{H}_2/\text{Ar}$ . Samples not annealed under reduced atmosphere were found to exhibit much weaker luminescence intensity, which may be attributed to the absence of  $\text{Eu}^{2+}$  and/or  $\text{Mn}^{2+}$ . The XRD patterns of  $\text{CaAl}_2\text{Si}_2\text{O}_8\text{:Eu, Mn}$  phases with different doping contents are shown in Figure 2 and all of the profiles were found to be in good agreement with that reported in JCPDS file 89-1462 regardless of the content of dopants and this observation indicates that no impurity phase is present.

Refinements of the XRD patterns for  $(\text{Ca}_{1-m-n}\text{Eu}_m\text{Mn}_n)\text{Al}_2\text{Si}_2\text{O}_8$  samples with different doping contents of  $\text{Mn}^{2+}$  indicated that the refined lattice parameters do not show significant change considering the standard deviations. Therefore, based on the effective ionic radii ( $r$ ) of cations with different coordination number ( $CN$ ) reported by Shannon,<sup>11</sup> we have proposed that  $\text{Eu}^{2+}$  and  $\text{Mn}^{2+}$  ions are expected to and, in fact, occupy the  $\text{Ca}^{2+}$  sites preferably, because the ionic radii of  $\text{Eu}^{2+}$  ( $r = 1.17$  Å when  $CN = 6$  and  $r = 1.20$  Å when  $CN = 7$ ) and  $\text{Mn}^{2+}$  ( $r = 0.83$  Å when  $CN = 6$  and  $r = 0.90$  Å when  $CN = 7$ ) are close to that of  $\text{Ca}^{2+}$  ( $r = 1.00$  Å when  $CN = 6$ ,  $r = 1.06$  Å when  $CN = 7$ ).<sup>11</sup> Since both four-coordinated  $\text{Al}^{3+}$  ( $r = 0.39$  Å) and  $\text{Si}^{4+}$  ( $r = 0.26$  Å) sites are too small for  $\text{Mn}^{2+}$  to occupy, we thereby conclude that  $\text{Mn}^{2+}$  ( $r = 0.66$  Å when  $CN = 4$ ) tends to prefer the  $\text{Ca}^{2+}$  sites due to size consideration.

The PL and PLE spectra for the purely  $\text{Eu}^{2+}$ -activated  $\text{CaAl}_2\text{Si}_2\text{O}_8$  are shown in Figure 3a. An intense broad band centered at 425 nm and attributed to the typical  $4f^65d^1(t_{2g}) \rightarrow 4f^7(^8S_{7/2})$  transition of  $\text{Eu}^{2+}$  was observed at ambient temperature. Furthermore, the PL and PLE for purely  $\text{Mn}^{2+}$ -activated  $\text{CaAl}_2\text{Si}_2\text{O}_8$  are represented in Figure 3b. The d-d transitions of  $\text{Mn}^{2+}$  are forbidden in spin and parity, so their excitation transitions are difficult to pump and emission intensity is very weak. The broad emission band centered at 568 nm is attributed to the spin-forbidden  $^4T_1(^4G) \rightarrow ^6A_1(^6S)$  transition of  $\text{Mn}^{2+}$ . The excitation spectrum consists of several bands centering at 340, 355, 403, 418, and 469 nm,

(9) Blasse, G. *Philips Res. Rep.* **1969**, *24*, 131.

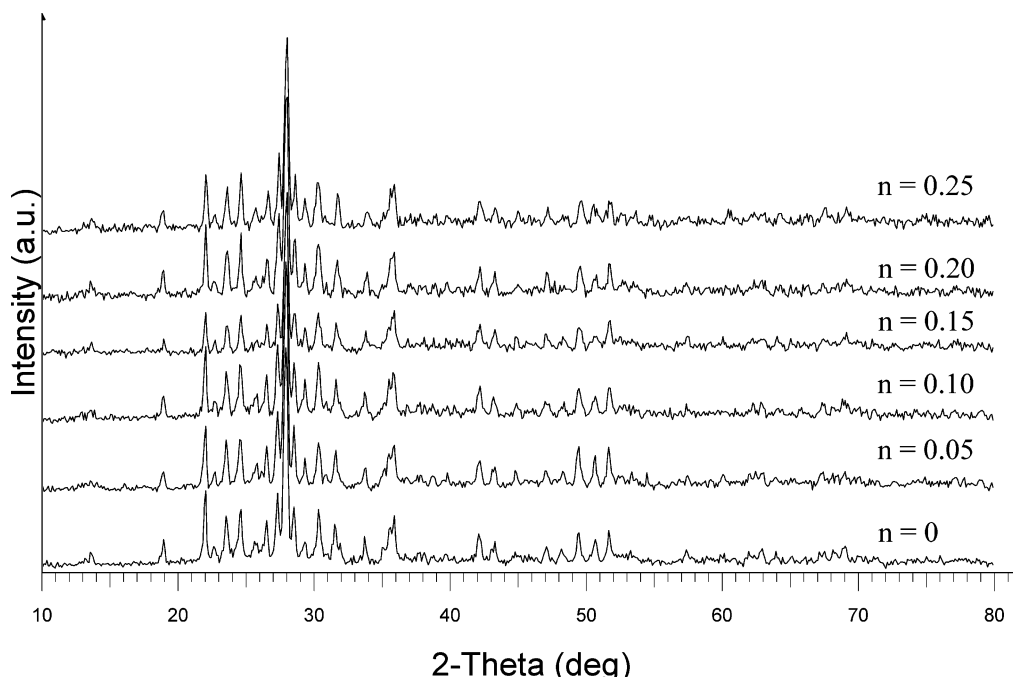


**Figure 2.** Dependence of XRD profiles for  $(\text{Ca}_{0.99-n}\text{Eu}_{0.01}\text{Mn}_n)\text{Al}_2\text{Si}_2\text{O}_8$  phosphors on  $\text{Mn}^{2+}$  doping content ( $n$ ).

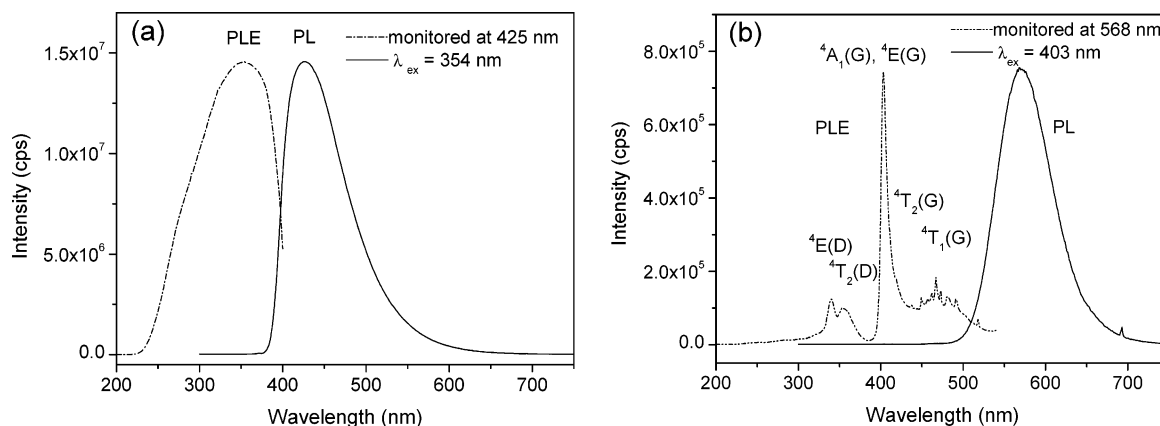


**Figure 3.** PLE and PL spectra for phosphors with compositions of  $\text{CaAl}_2\text{Si}_2\text{O}_8:0.01\text{Eu}^{2+}$  (a) and  $\text{CaAl}_2\text{Si}_2\text{O}_8:0.25\text{Mn}^{2+}$  (b).

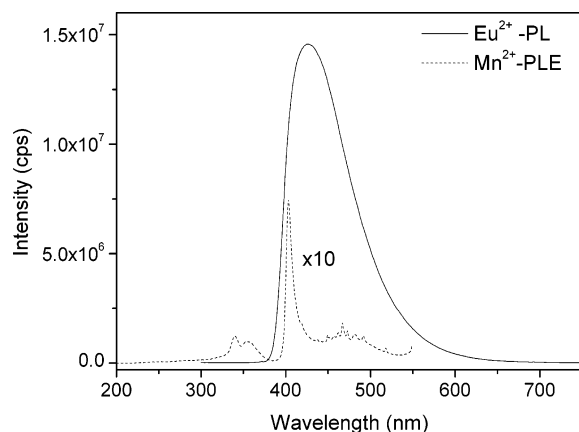


**Figure 4.** Spectral overlap between the PL spectrum of  $(\text{Ca}_{0.99}\text{Eu}_{0.01})\text{Al}_2\text{Si}_2\text{O}_8$  (solid line) and PLE spectrum of  $(\text{Ca}_{0.75}\text{Mn}_{0.25})\text{Al}_2\text{Si}_2\text{O}_8$  (dashed line).

corresponding to the transitions from  $^6\text{A}_1(^6\text{S})$  to  $^4\text{E}(^4\text{D})$ ,  $^4\text{T}_2(^4\text{D})$ ,  $[\text{}^4\text{A}_1(^4\text{G}), \text{}^4\text{E}(^4\text{G})]$ ,  $^4\text{T}_2(^4\text{G})$ , and  $^4\text{T}_1(^4\text{G})$  levels, respectively.

As shown in Figure 3a and b and Figure 4, the comparison of the PL and PLE spectra for  $\text{CaAl}_2\text{Si}_2\text{O}_8:\text{Eu}$  and  $\text{CaAl}_2\text{Si}_2\text{O}_8:\text{Mn}$  phosphors reveals a significant spectral overlap

between the emission band of  $\text{Eu}^{2+}$  centered at 425 nm and the  $\text{Mn}^{2+}$  excitation transitions of  $^6\text{A}_1(^6\text{S}) \rightarrow ^4\text{T}_1(^4\text{G})$ ,  $^4\text{T}_2(^4\text{G})$ ,  $[\text{}^4\text{A}_1(^4\text{G}), \text{}^4\text{E}(^4\text{G})]$ . Therefore, the effective resonance-type energy transfer from  $\text{Eu}^{2+}$  to  $\text{Mn}^{2+}$  is expected. This type of energy transfer is quite common and has been observed in several  $\text{Eu}^{2+}$ - and  $\text{Mn}^{2+}$ -coactivated phosphors such as  $\text{CaCl}_2:\text{Eu}, \text{Mn}$ ,<sup>2</sup>  $\text{KBr}:\text{Eu}, \text{Mn}$ ,<sup>6</sup>  $\text{BaMg}_2\text{Si}_2\text{O}_7:\text{Eu}, \text{Mn}$ ,<sup>4</sup> and  $\text{Ba}_3\text{MgSi}_2\text{O}_8:\text{Eu}, \text{Mn}$ ,<sup>7</sup> respectively.

Figure 5 shows the PLE and PL spectra for six  $\text{Eu}^{2+}$  and  $\text{Mn}^{2+}$ -coactivated  $(\text{Ca}_{0.99-n}\text{Eu}_{0.01}\text{Mn}_n)\text{Al}_2\text{Si}_2\text{O}_8$  phosphors with different dopant contents  $n$  of 0, 0.05, 0.10, 0.15, 0.20, and 0.25, respectively. The PLE spectra monitored at 425 nm ( $\text{Eu}^{2+}$  emission) show an optimal excitation band centered at 354 nm, which consists of unresolved bands due to the  $4f5d$  multiplets of the  $\text{Eu}^{2+}$  excited state. Interestingly and reasonably, the PL intensity of  $\text{Mn}^{2+}$  activator (or energy acceptor) was observed to increase, whereas that of  $\text{Eu}^{2+}$  sensitizer (or energy donor) is simultaneously found to decrease monotonically with increasing  $\text{Mn}^{2+}$  dopant content. The dependence of the relative emission intensity of  $\text{Eu}^{2+}$  on different  $\text{Mn}^{2+}$  dopant content ( $n$ ) is represented in Figure

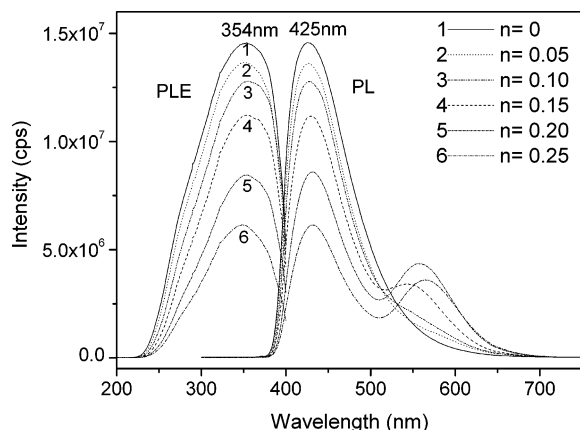


**Figure 5.** PLE and PL spectra for  $(\text{Ca}_{0.99-n}\text{Eu}_{0.01}\text{Mn}_n)\text{Al}_2\text{Si}_2\text{O}_8$  phosphors (PLE monitored at 425 nm and PL excited at 354 nm).

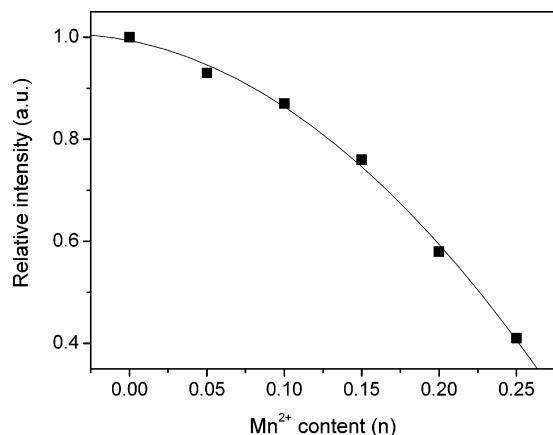


**Figure 6.** Dependence of the relative emission intensity of  $\text{Eu}^{2+}$  in  $(\text{Ca}_{0.99-n}\text{Eu}^{2+}_{0.01}\text{Mn}^{2+}_n)\text{Al}_2\text{Si}_2\text{O}_8$  on  $\text{Mn}^{2+}$  content  $n$ .

6. The PL intensity of  $\text{Eu}^{2+}$  emission band was found to decrease monotonically with increasing doped  $\text{Mn}^{2+}$  concentration. Similar observations reported by Yamashita et al.<sup>12</sup> and Ruelle et al.<sup>13</sup> is attributed to the formation of paired  $\text{Mn}^{2+}$  centers with faster decay than single  $\text{Mn}^{2+}$  centers.

The PL decay curves of  $\text{Eu}^{2+}$  in  $(\text{Ca}_{0.99-n}\text{Eu}^{2+}_{0.01}\text{Mn}^{2+}_n)\text{Al}_2\text{Si}_2\text{O}_8$  were measured and are represented in Figure 7. As described by Blasse and Grabmaier,<sup>14</sup> it is well established that the decay behavior of  $\text{Eu}^{2+}$  can be expressed by

$$I = I_0 \exp(-t/\tau) \quad (1)$$

, where  $I$  and  $I_0$  are the luminescence intensities at time  $t$  and 0, and  $\tau$  is the luminescence lifetime. On the basis of eq 1 and decay curves, the lifetime values were determined to be 0.73, 0.66, 0.57, 0.43, and  $0.34 \mu\text{s}$  for  $(\text{Ca}_{0.99-n}\text{Eu}_{0.01}\text{Mn}_n)\text{Al}_2\text{Si}_2\text{O}_8$  with  $n = 0, 0.10, 0.15, 0.20$ , and  $0.25$ , respectively. The decay lifetime for  $\text{Eu}^{2+}$  was found to decrease with increasing  $\text{Mn}^{2+}$  dopant content, which is strong evidence for the energy transfer from  $\text{Eu}^{2+}$  to  $\text{Mn}^{2+}$ , as reported by Ruelle et al.<sup>13</sup> and Jiao et al.,<sup>15</sup> respectively.

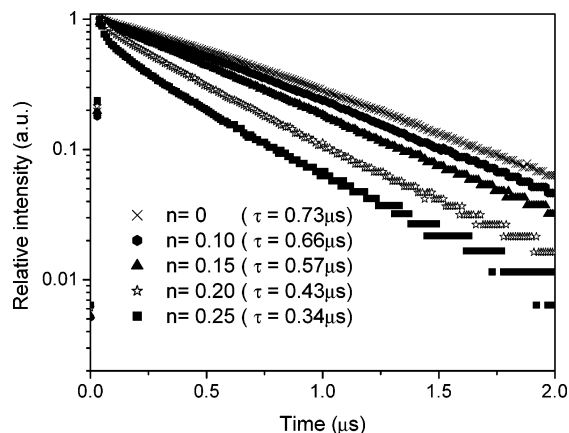


**Figure 7.** Photoluminescence decay curve of  $\text{Eu}^{2+}$  in  $(\text{Ca}_{0.99-n}\text{Eu}^{2+}_{0.01}\text{Mn}^{2+}_n)\text{Al}_2\text{Si}_2\text{O}_8$  (excited at 355 nm, monitored at 425 nm).

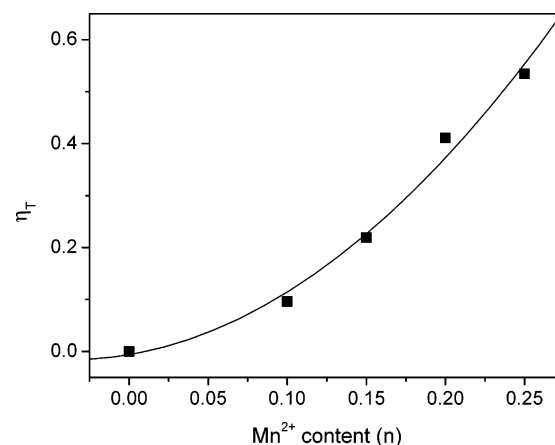


**Figure 8.** Dependence of the energy transfer efficiency  $\eta_T$  in  $(\text{Ca}_{0.99-n}\text{Eu}^{2+}_{0.01}\text{Mn}^{2+}_n)\text{Al}_2\text{Si}_2\text{O}_8$  on  $\text{Mn}^{2+}$  content  $n$ .

We are also interested in investigating the energy transfer efficiency ( $\eta_T$ ) of  $\text{Eu}^{2+} \rightarrow \text{Mn}^{2+}$  and a simple operational definition as suggested by Paulose et al.,<sup>16</sup>  $\eta_T$  can be expressed by

$$\eta_T = 1 - \frac{\tau_S}{\tau_{S0}} \quad (2)$$

where  $\tau_{S0}$  is the intrinsic decay lifetime of the sensitizer ( $\text{Eu}^{2+}$ ) and  $\tau_S$  is the decay lifetime of the sensitizer ( $\text{Eu}^{2+}$ ) in the presence of the activator ( $\text{Mn}^{2+}$ ). The energy transfer efficiency for  $\text{Eu}^{2+} \rightarrow \text{Mn}^{2+}$  in  $(\text{Ca}_{0.99-n}\text{Eu}^{2+}_{0.01}\text{Mn}^{2+}_n)\text{Al}_2\text{Si}_2\text{O}_8$  was calculated and is illustrated in Figure 8. With increasing  $\text{Mn}^{2+}$  dopant content, the energy transfer efficiency  $\eta_T$  was found to increase gradually.

According to Dexter and Schulman, concentration quenching is in many cases due to energy transfer from one activator to another until an energy sink in the lattice is reached.<sup>17</sup> As suggested by Blasse,<sup>9</sup> the average separation  $R_{\text{Eu-Mn}}$  can be expressed by

$$R_{\text{Eu-Mn}} = 2 \left[ \frac{3V}{4\pi xN} \right]^{1/3} \quad (3)$$

(10) Altermatt, U. D.; Brown, I. D. *Acta Crystallogr.* **1987**, A34, 125.

(11) Shannon, R. D. *Acta Crystallogr.* **1976**, A32, 751.

(12) Yamashita, N.; Maekawa, S.; Nakamura, K. *Jpn. J. Appl. Phys.* **1990**, 29, 1729.

(13) Ruelle, N.; Pham-Thi, M.; Fouassier, C. *Jpn. J. Appl. Phys.* **1992**, 31, 2786.

(14) Blasse, G.; Grabmaier, B. C. *Luminescent Materials*; Springer-Verlag: Berlin, Germany, 1994; p 96.

(15) Jiao, H.; Liao, F.; Tian, S.; Jing, X. *J. Electrochem. Soc.* **2003**, 150, H220.

(16) Paulose, P. I.; Jose, G.; Thomas, V.; Unnikrishnan, N. V.; Warriar, M. K. R. *J. Phys. Chem. Solids* **2003**, 64, 841.



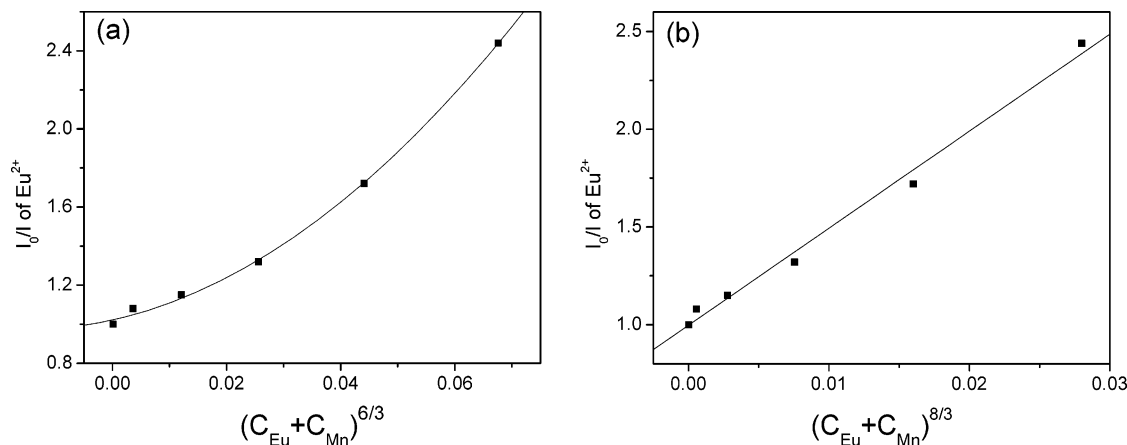


**Figure 9.** Dependence of  $I_0/I_S$  of  $\text{Eu}^{2+}$  on (a)  $C^{6/3}$  and (b)  $C^{8/3}$ .

where  $N$  is the number of Z ions in the unit cell, and  $V$  is the volume of the unit cell. For  $\text{CaAl}_2\text{Si}_2\text{O}_8$  host,  $N = 8$  and  $V = 1337.8 \text{ \AA}^3$ .  $x$  is the total concentration of  $\text{Eu}^{2+}$  and  $\text{Mn}^{2+}$ . Thus,  $R_{\text{Eu-Mn}}$  (in  $\text{\AA}$ ) is determined to be 17.5, 14.3, 12.6, 11.5, and 10.7 for  $n = 0.05, 0.10, 0.15, 0.20$ , and  $0.25$ , respectively, in  $(\text{Ca}_{0.99-n}\text{Eu}_{0.01}\text{Mn}_n)\text{Al}_2\text{Si}_2\text{O}_8$ . The critical concentration  $x_c$ , at which the luminescence intensity of  $\text{Eu}^{2+}$  is half that in the sample in the absence of  $\text{Mn}^{2+}$ , is 0.24. Therefore, the critical distance ( $R_c$ ) of energy transfer was calculated to be about 11.0  $\text{\AA}$ . We have also observed that the radiative emission from  $\text{Eu}^{2+}$  prevails when  $R_{\text{Eu-Mn}} > R_c$  and energy transfer from  $\text{Eu}^{2+}$  to  $\text{Mn}^{2+}$  dominates when  $R_{\text{Eu-Mn}} < R_c$ .

On the basis of Dexter's energy transfer formula of multipolar interaction and Reisfeld's approximation the following relation can be obtained<sup>15,18,19</sup>

$$\frac{\eta_0}{\eta} \propto C^{n/3} \quad (4)$$

where  $\eta_0$  and  $\eta$  are, respectively, the luminescence quantum efficiency of  $\text{Eu}^{2+}$  in the absence and presence of  $\text{Mn}^{2+}$ ;  $C$  is the sum of the content of  $\text{Eu}^{2+}$  and  $\text{Mn}^{2+}$ ;  $n = 6, 8$ , and  $10$ , corresponding to dipole–dipole, dipole–quadrupole, and quadrupole–quadrupole interactions, respectively. The value  $\eta_0/\eta$  is approximately calculated by the ratio of related luminescence intensities as<sup>15,17</sup>

$$\frac{I_{S0}}{I_S} \propto C^{n/3} \quad (5)$$

, where  $I_{S0}$  is the intrinsic luminescence intensity of  $\text{Eu}^{2+}$  and  $I_S$  is the luminescence intensity of  $\text{Eu}^{2+}$  in the presence of the  $\text{Mn}^{2+}$ . The  $I_{S0}/I_S - C^{n/3}$  plot is represented in Figure 9a and b, and only when  $n = 8$  does it show linear relation. This clearly indicates that the energy transfer from  $\text{Eu}^{2+}$  to  $\text{Mn}^{2+}$  is the dipole–quadrupole mechanism.

For dipole–quadrupole mechanism, the transfer probability is given by Dexter<sup>9,20</sup> as

$$P_{\text{Eu-Mn}}^{DQ} = 0.63 \times 10^{28} \frac{f_q \lambda_s^2 Q_A}{\tau_{S0} f_d R_{\text{Eu-Mn}}^8 E_S^4} \int F_S(E) F_A(E) dE \quad (6)$$

where  $Q_A = 4.8 \times 10^{-16} f_d$  is the absorption cross-section of  $\text{Mn}^{2+}$ ,  $f_d = 10^{-7}$  and  $f_q = 10^{-10}$  are the oscillator strengths

of dipole and quadrupole electrical absorption transitions for  $\text{Mn}^{2+}$ ;  $\lambda_s$  (in  $\text{\AA}$ ) and  $E$  (in eV) are emission wavelength and emission energy of  $\text{Eu}^{2+}$ ;  $\int F_S(E) F_A(E) dE$  represents the spectral overlap between the normalized shapes of the  $\text{Eu}^{2+}$  emission  $F_S(E)$  and  $\text{Mn}^{2+}$  excitation  $F_A(E)$ , and it is estimated at about  $2.39 \text{ eV}^{-1}$ .

The critical distance ( $R_c$ ) of energy transfer from  $\text{Eu}^{2+}$  to  $\text{Mn}^{2+}$  is defined as the distance for which the probability of transfer equals the probability of radiative emission of  $\text{Eu}^{2+}$ , i.e., the distance for which  $P_{\text{Eu-Mn}} \tau_{S0} = 1$ . Therefore,  $R_c$  can be found from eq 6

$$R_c^8 = 0.63 \times 10^{28} \frac{f_q \lambda_s^2 Q_A}{f_d E_S^4} \int F_S(E) F_A(E) dE \quad (7)$$

In this system, the critical distance of energy transfer was calculated to be about 10.8  $\text{\AA}$ . This result is in good agreement with that obtained using the concentration quenching method.

As we know, the PLE spectrum is comparable to an absorption spectrum, the single excitation band centered at ca. 354 nm in the PLE spectra can be reasonable referred to one absorption process. To investigate the energy absorption of the aluminosilicate phosphors, diffuse reflectance spectra for parent and doped  $\text{CaAl}_2\text{Si}_2\text{O}_8$  phosphors were measured and are shown in Figure 10. As indicated in Figure 10, for parent  $\text{CaAl}_2\text{Si}_2\text{O}_8$  an increase of reflectance from 275 to 345 nm was noted. The middle points at ca. 311 nm may be used to estimate the approximate band gap of host material  $\text{CaAl}_2\text{Si}_2\text{O}_8$ . Furthermore, the reflectance spectra for  $(\text{Ca}_{0.99-n}\text{Eu}_{0.01}\text{Mn}_n)\text{Al}_2\text{Si}_2\text{O}_8$  phases with  $n = 0, 0.10, 0.15, 0.20$ , and  $0.25$  show extreme resemblance with a decrease of reflectance at 375 nm. On the other hand, reflectance spectra for  $(\text{Ca}_{0.75}\text{Mn}_{0.25})\text{Al}_2\text{Si}_2\text{O}_8$  phase exhibit two slight changes at 275 and 380 nm, respectively, which may be attributed to the energy absorption feature of the host material.

In an attempt to investigate the chromaticity of the phosphors as a function of dopant contents, we have prepared

(17) Dexter, D. L.; Schulman, J. A. *J. Chem. Phys.* **1954**, *22*, 1063.

(18) Reisfeld, R.; Lieblich-sofer, N. *J. Solid State Chem.* **1979**, *28*, 391.

(19) Bijju, P. R.; Jose, G.; Thomas, V.; Nampoori, V. P. N.; Unnikrishnan, N. V. *Opt. Mater.* **2004**, *24*, 671.

(20) Dexter, D. L. *J. Chem. Phys.* **1953**, *21*, 836.

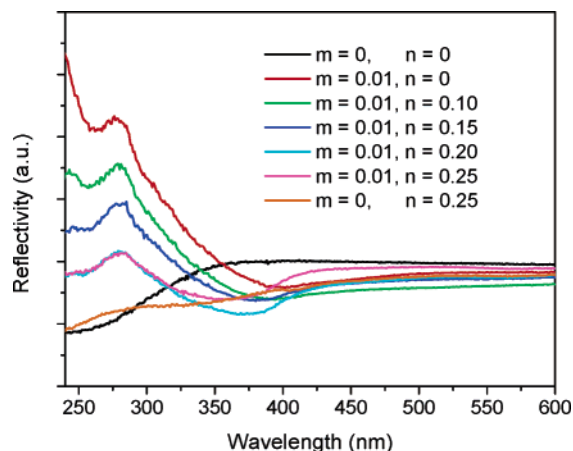


**Figure 10.** Reflectance spectra for  $\text{Eu}^{2+}$ - and  $\text{Mn}^{2+}$ -activated and  $\text{Eu}^{2+}/\text{Mn}^{2+}$ -coactivated  $\text{CaAl}_2\text{Si}_2\text{O}_8$  phosphors.

**Table 1.** Comparison of CIE Chromaticity Coordinates for  $(\text{Ca}_{0.99-n}\text{Eu}_{0.01}\text{Mn}_n)\text{Al}_2\text{Si}_2\text{O}_8$  ( $\lambda_{\text{ex}} = 354$  nm) and Simulated White Light Using Commercial  $\text{Y}_3\text{Al}_5\text{O}_{12}:\text{Ce}$  Phosphors ( $\lambda_{\text{ex}} = 467$  nm)

sample	(x, y)
$n = 0$	(0.17, 0.11)
$n = 0.05$	(0.18, 0.12)
$n = 0.10$	(0.20, 0.14)
$n = 0.15$	(0.24, 0.21)
$n = 0.20$	(0.30, 0.29)
$n = 0.25$	(0.33, 0.31)
simulated white light with $\text{Y}_3\text{Al}_5\text{O}_{12}:\text{Ce}$	(0.31, 0.27)

a series of  $(\text{Ca}_{0.99-n}\text{Eu}_{0.01}\text{Mn}_n)\text{Al}_2\text{Si}_2\text{O}_8$  phosphors with  $n = 0, 0.05, 0.10, 0.15, 0.20$ , and  $0.25$ , respectively. Table 1 summarizes the comparison of CIE chromaticity coordinates for  $(\text{Ca}_{0.99-n}\text{Eu}_{0.01}\text{Mn}_n)\text{Al}_2\text{Si}_2\text{O}_8$  as a function of  $\text{Mn}^{2+}$  content ( $\lambda_{\text{ex}} = 354$  nm), simulated white-light using commercial  $\text{Y}_3\text{Al}_5\text{O}_{12}:\text{Ce}$  phosphors ( $\lambda_{\text{ex}} = 467$  nm), and  $\text{Y}_3\text{Al}_5\text{O}_{12}:\text{Ce}$  itself. The chromaticity coordinates for  $(\text{Ca}_{0.99-n}\text{Eu}_{0.01}\text{Mn}_n)\text{Al}_2\text{Si}_2\text{O}_8$  are represented as series A in Figure 11. We have observed that the (x,y) coordinates vary systematically from (0.17, 0.11) to (0.33, 0.31), and corresponding hue of the samples varied gradually from blue, aqua, and eventually to white, as we vary the dopant contents of  $\text{Mn}^{2+}$  from  $n = 0$  to 0.25, as indicated in the chromaticity diagram. Furthermore, to evaluate the potential of our tunable aluminosilicates as white-emitting phosphors, we have investigated and compared the chromaticity characteristics of the simulated white light generated from commercial YAG:Ce (Nichia Co., Japan) that was excited with monochromatic blue light of 467 nm with coordinates of (0.15, 0.04). As represented as series B in Figure 11, the experimentally determined chromaticity coordinates were found to be (0.48, 0.50) for YAG:Ce and (0.31, 0.27) for the simulated white light, the color saturation of which was found to be inferior to that generated from our phosphor. In practice, with increasing the amount of electrical current, the hue of a white-light LED changes from yellow to white and to blue. Therefore, the white-light LED of YAG:Ce excited by blue-light chip tends

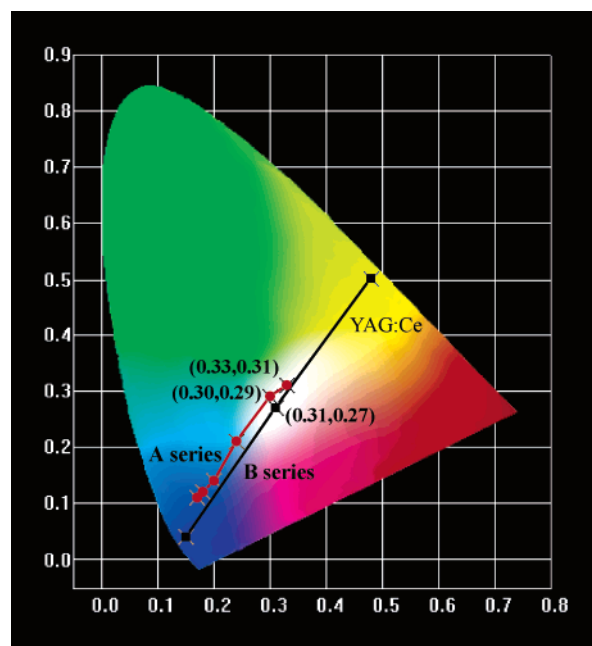


**Figure 11.** CIE chromaticity diagram for  $(\text{Ca}_{0.99-n}\text{Eu}_{0.01}\text{Mn}_n)\text{Al}_2\text{Si}_2\text{O}_8$  phosphors with different  $\text{Mn}^{2+}$  dopant contents ( $\lambda_{\text{ex}} = 354$  nm) (series A) and simulated white light generated with YAG:Ce (Nichia Co.) ( $\lambda_{\text{ex}} = 467$  nm) (series B).

to produce color aberration when the LED chip is degrading. In contrast, our  $\text{CaAl}_2\text{Si}_2\text{O}_8:\text{Eu}^{2+}, \text{Mn}^{2+}$  phosphors excited with ultraviolet light will not have that problem because the excited light is invisible. The above observations hint the promising application of  $(\text{Ca}_{0.99-n}\text{Eu}_{0.01}\text{Mn}_n)\text{Al}_2\text{Si}_2\text{O}_8$  phases as a white-emitting phosphor for ultraviolet LEDs.

#### 4. Conclusions

In summary, we have synthesized and investigated the luminescent properties of  $\text{CaAl}_2\text{Si}_2\text{O}_8$  phosphors coactivated with  $\text{Eu}^{2+}$  and  $\text{Mn}^{2+}$  under photoexcitation. The spectroscopic data indicate that the  $\text{Eu}^{2+} \rightarrow \text{Mn}^{2+}$  energy transfer process takes place in the host matrix of  $\text{CaAl}_2\text{Si}_2\text{O}_8$ . The energy transfer from  $\text{Eu}^{2+}$  to  $\text{Mn}^{2+}$  has found to occur via a dipole–quadrupole mechanism. The critical energy transfer distance has also been calculated by the concentration quenching and spectral overlap methods. The results obtained from the two approaches are in good agreement. Furthermore, we have also demonstrated that the  $(\text{Ca}_{0.99-n}\text{Eu}_{0.01}\text{Mn}_n)\text{Al}_2\text{Si}_2\text{O}_8$  can be systematically tuned to generate white light under ultraviolet radiation and it has been shown to exhibit the potential to act as a white-emitting phosphor for ultraviolet LEDs.

**Acknowledgment.** We acknowledge generous financial support from the National Science Council of Taiwan, R.O.C. under contracts NSC92-2113-M009-019 and NSC93-2113-M009-009.

CM050638F